NUMERICAL MODELING OF ICE-STRUCTURE INTERACTION

Quarterly Progress Report No. 4

September 30, 1985 - December 31, 1985

Research Supported By
MINERALS MANAGEMENT SERVICE
United States Department of the Interior

Contract No. 14-12-0001-30219
Duration of Contract: 09/28/1984 - 09/30/1987
Contract Amount: $110,000
COTR: Mr. Charles E. Smith

Prepared By
Prof. S. Shyam Sunder - Principal Investigator
Prof. Jerome J. Connor - Co-Principal Investigator

Department of Civil Engineering
MASSACHUSETTS INSTITUTE OF TECHNOLOGY
Room 1-274
Cambridge, Massachusetts 02139

January 1, 1986

TABLE OF CONTENTS

1. INTRODUCTION

OBJECTIVE OF PROPOSED WORK

The objective of this project is to systematically investigate using numerical models the mechanics of deformation and progressive failure in ice for the purpose of predicting global forces and local pressures on offshore structures proposed for deployment in the Arctic. The focus is on ice sheets interacting with rigid cylindrical indenters. The project involves the following three major areas of study:

1. Development of constitutive models to characterize the mechanical behavior of sea ice.
2. Development of finite element methods of analysis to account for the simultaneous occurrence of viscous (rate dependent) and fracture behavior in ice, and time varying contact between ice and structure.
3. Numerical solution of ice-structure interaction processes for selected ice features and structural configurations to predict global forces and local pressures.

BACKGROUND

As much as 30-40 percent of the U.S. undiscovered hydrocarbon recoverable reserves, comparable in magnitude to those of the Persian Gulf, are estimated to lie in the Arctic. The extraction of these resources in an economical and safe manner poses many technical challenges to offshore engineering. At the root of these problems is the severe environment created by perennial ice features that impart global forces and local pressures on structures which are several times greater than those from waves

in non-Arctic environments. Typically, two levels of ice loading are considered for design purposes. Global ice loads govern the overall structural geometry and dimensions as well as the foundation design, while local ice pressures are likely to dictate wall thicknesses and local framing, and may well govern structural cost.

Most of the emphasis in research has been on predicting global forces. Only during recent years, as the focus changed from overall feasibility to preliminary and detailed design, has the importance of local pressures emerged. It is widely recognized that significant uncertainties exist in the ice load models in use today and that some design loads may be overestimated by an order of magntidue. Research is necessary to quantify the uncertainties in ice loads and to develop improved load prediction models for the safe and economical design of structures.

Uncertainties in existing ice load models arise primarily from five sources:

- Incomplete modeling of the mechanical behavior of ice, including temperature and fracture effects.
- Empiricism in existing theoretical models resulting from the use of approximate analysis methods.
- Inadequate modeling of the contact forces at the ice-structure interface.
- Neglecting the effect of scale/size on material strength.
- Not accounting for the finiteness of environmental and other forces driving the ice features.

In order to quantify these uncertainties and to better predict global and local ice loads, numerical models are necessary for computer simulation

of ice-structure interaction processes. In contrast to analytical methods, such models can realistically simulate the interaction accounting for spatial-temporal variability in the mechanical behavior of ice and for multiple modes of failure in ice.

The complexity of sea ice behavior is due mainly to:

- Strong dependence on rate of loading, which is spatially and temporally variable in ice features.
- Simultaneous occurrence of ductile, strain-softening, and brittle modes of deformation.
- Pressure sensitivity leading to different strengths in compression and tension (at moderate-to-high rates of loading) and to melting point depression.
- Material anisotropy leading to strength variation by a factor of three.
- Strong dependence on temperature, varying in first year ice from melting point at the water interface to perhaps -50°F at the air interface.
- Strong dependence on internal structure of ice (grain size, fabric, brine volume, salinity, porosity), which is spatially varying particularly in multi-year ice features.

A key aspect in the development of constitutive models is the need for accurate and consistent experimental data on ice, especially to characterize its behavior relating to tensile loading, cyclic loading, multiaxial loading, nucleation and interaction of cracks, material anisotropy, thermal and structural gradients, and fracture toughness. Currently available data is in many cases sufficient to postulate approximate constitutive models.

Numerical simulations can help to establish the importance of more extensive experimentation in quantifying ice-structure interaction processes.

Finite element methods of analysis for simulating ice-structure interaction processes are affected by the following research concerns:

- Rate dependent material behavior with negligible elastic deformation.
- Initiation and propagation of cracks due to fracture.
- Simultaneous occurrence of rate dependent and fracture behavior.
- Adfreeze bond and friction at ice-structure interface.
- Time-varying contact between ice and stucture and between fractured ice features.
- Strain-softening of ice.

STAFFING

Dr. S. Shyam Sunder, Winslow Associate Professor of Civil Engineering, is Principal Investigator for this project while Dr. Jerome J. Connor, Professor of Civil Engineering, is Co-Principal Investigator. In addition, two full-time graduate Research Assistants are participating in this research. They are Mr. S-K Ting, a doctoral student with considerable experience in concrete testing and dynamic behavior of offshore structures (9/1/84 - 10/31/85); Mr. F.S. Chehayeb, a doctoral student whose background is in numerical analysis and finite element methods (9/1/84 -5/31/85); Mr. J. Ganguly, a master's student with expertise in computational mechanics (6/1/85 - 1/15/86), and Mr. C-W. Chen, a doctoral student with strong background in computational mechanics and many years of professional experience in the nuclear power industry (1/1/86-5/31/86). Mr. Ting successfully defended his doctoral thesis in October 1985.

2. SUMMARY OF RESEARCH ACTIVITIES

The principal technical developments through the end of this reporting period have been:

(1) The study of sea ice indentation in the creeping mode of deformation.

(2) Initiation of research to study sea ice indentation accounting for fracture behavior.

Specific accomplishments and current research directions are discussed below.

SEA ICE INDENTATION IN THE CREEPING MODE

A study of ice indentation in the creeping mode is important for two reasons: (a) creep is the predominant mode of deformation for artificial islands in the Arctic nearshore region during "breakout" and/or steady indentation conditions occurring in the winter, and (b) stresses, strains, and strainrates within the continuum resulting from creep are necessary to predict the nucleation, growth initiation and propagation of cracks when viscous effects influence fracture. The latter scenario, which defines the transition from ductile to brittle behavior, may represent the most severe loading case since indentation pressures tend to be lower at very fast ice movement rates.

Global and local pressures generated during sea ice indentation in the creeping mode are being studied, accounting for the spatial variation of strainrates. Two methods of analysis are being considered: (a) approximate methods, i.e., upper-bound method and strain path method, and (b) "exact" method based on the finite element method. In both cases, a two-dimensional idealization of the indentation process is considered. In order to provide

continuity with previous work, the isotropic, incompressible three-dimensional extension of the uniaxial power-law creep model for ice has been extensively studied. Pressures predicted with this model, and an orthotropic generalization which accounts for material anisotropy, are being compared with those from previously published formulas. In addition, ice pressures have been obtained with the approximate methods for a new uniaxial model that accounts for the stress-strain-strainrate behavior of sea ice, including its strain-softening behavior.

The key difference in the two approximate methods of analysis is that point stresses within the continuum can be obtained with the strain path method. As a result, local stresses at the ice-structure interface can be estimated, unlike the upper bound method which only yields the global pressure. However, both methods rely on an adequate specificiation of the velocity field in the ice sheet. This is obtained through a combination of theoretical modeling based on fluid mechanics and field ice movement survey data from an artificial island in the Beaufort Sea. In particular, two theoretical kinematic models are considered: one resulting from the superposition of a point source and a uniform flow (Kinematic Model A) that has been proposed by Bruen & Vivatrat; and the other resulting from the superposition of a doublet and a uniform flow (Kinematic Model B).

The results of the approximate methods indicate that:

(a) Kinematic Model B better models the ice movement survey data used here than Kinematic Model A.

(b) In the creeping mode of ice deformation, local ice pressures are of the same order of magnitude as the global pressures.

(c) Under the same conditions, Kinematic Model B, the API model, and the Ponter et al. model predict similar global pressures.

(d) The variation in global pressures for different power-law model parameters (Wang, Sanderson, Ting & Shyam Sunder) is on the order of 30%.

A key finding of the work is that for rate-dependent material models describing sea ice behavior, interface adfreeze and friction stresses can significantly influence both local and global ice pressures. The only realistic way to study these effects is through numerical models based on the finite element method of analysis.

This research has been summarized in a paper entitled "Sea Ice Indentation Accounting for Strain-Rate Variation", published in the proceedings of the ASCE Specialty Conference: ARCTIC '85 - Civil Engineering in the Arctic Offshore held at San Francisco, CA, March 25-27, 1985.

A finite element formulation for general viscoplastic behavior including creep (nonlinear viscoelasticity) has been developed and implemented in a computer code called DECNEC (Discrete Element Computational NEtwork Controller). A new bi-level solution algorithm has been developed for fast convergence in problems where permanent deformations dominate. This algorithm is based on a secant type iteration on the global equations of motion and a Newton-Raphson (tangent type) iteration, combined with an implicit numerical time integrator, on the rate-dependent constitutive relations at each integration point within an element. A post-processor, originally written at the Lawrence Livermore Laboratory, can be used in conjunction with the computer code to produce graphical displays. The program has the ability to simulate a fixed, roller, free or frictional contact between two deformable bodies. The fixed condition represents an infinitely strong interface, the free condition corresponds to no adfreeze bond strength or frictional stresses, while the roller condition provides an

intermediate solution. The current implementation is a two-dimensional version for plane stress problems. A four noded quadrilateral element is currently available. Although an eight-noded quadratic element is often preferred (and may be included in the future), accurate results are obtained with the four-noded element using a finer finite element mesh.

The accuracy of the computer code has been verified in two ways; through the solution of simple test problems, and by comparing the variability in predicted global pressures due to indenter diameter, material model parameters, and ice sheet velocity with that predicted by approximate methods of analysis. In both cases, the numerical solutions are accurate to within specified tolerances typically achievable in finite element analyses.

Numerical simulations have been performed under plane stress conditions to assess the influence of interface adfreeze and friction, variability in material constants for an isotropic multi-axial power law creep model, rubble pile or grounded ice foot, and ice sheet velocity on global forces and local pressures generated on a rigid cylindrical indenter. The results have been compared with those based on approximate methods of analysis. Stress, strainrate, and strain countours have been obtained in addition to the distribution of interface pressures.

The numerical simulations show that:

1. Global forces vary by a factor of 2.5 depending upon whether the interface condition is fixed (infinite adfreeze bond strength), roller, or free (no adfreeze bond strength or interface friction). The fixed condition is about 1.3 times and the free condition about 0.5 times the roller condition.

2. Finite element analysis predictions of global pressure differ from a modified form of the upper bound solution for Kinematic Model B by less than 10% for varying velocity, indenter diameter, and material constants. The modification is necessary since the two-dimensional nature of the kinematic models makes the approximate solutions strictly apply to plane strain conditions, and not to the plane stress condition of interest.
3. The ratio of maximum normal interface pressure to global pressure approximately varies in the range 0.36-1.16 depending upon the interface condition. It is 0.36 for the fixed condition, 0.56 for the roller condition, and 1.16 for the free condition.
4. The maximum (peak) normal interface pressures vary by a factor of 1.26 depending upon the interface condition. The fixed condition is about 0.83 times and the free condition about 1.04 times the roller condition. The maximum interface shear stress for the fixed condition is about 0.81 times the corresponding maximum normal pressure. However, a different boundary value problem involving a smaller contact area, as opposed to contact over half the perimeter in the free condition, will lead to higher interface pressures.
5. Pressure-area curves should be considered as providing the maximum normal interface pressure for a given indenter area of contact (form area), rather than the average integrated normal pressure over a tributary loaded area for a structural component. It is conservative to assume a uniform or rectangular distribution of the local pressure over the indenter area of contact for purposes of design.

6. Tensile stresses, strains and strainrates occur almost all over the ice sheet, and may be the key to explaining fracture behavior during indentation. While biaxial compression and tension states tend to occur for stress on the upstream and downstream sides, respectively, the state of strain is almost always compression-tension. The levels of tensile strain are often sufficient to cause cracking even before steady state creep is reached.

The possible effect of a grounded rubble pile or accreted ice foot on ice pressures was assessed by defining an effective indenter equal to a multiple (2.86) of the structural diameter. This resulted in a factor of 1.97 to 1.99 increase in global force. In the case of a grounded rubble pile, it would be over conservative to consider that all this force is transmitted to the foundation by the structure. On the other hand, the force transmitted to the foundation by the structure would decrease by a factor of about four if both the structure and the grounded rubble pile could transmit a force proportional to the contact area of each with the foundation. This may be reasonable only if the rubble pile is consolidated and grounded fimly in the foundation soil such as in the case of constructed ice packs. Further research is necessary to quantify the level of force that can be directly transmitted to the foundation by a grounded rubble pile.

The numerical simulations also showed that (i) even a factor of two uncertainty in velocity will affect ice pressures only by about 20-30%, and (ii) uncertainties in material constants for an isotropic power law creep model may yield ice pressures that vary by about 15-30%, but natural variability in sea ice strength can have a significant influence on the

pressures. However, improved material models that include fracture and temperature effects in addition to the transversely isotropic behavior of sheet ice can have a major influence on ice pressure predictions.

This research has been summarized in a paper entitled "Sea Ice Indentation in the Creeping Mode", published in the proceedings of the 17th Annual Offshore Technology Conference, Houston, TX, May 6-9, 1985.

Sea ice, however, is not an isotropic material. Field observations have shown that this type of ice, which is predominantly columnar, has two sources of anisotropy: (a) the c-axis is oriented perpendicular to the axis of crystal growth, and (b) the c-axes of different crystals may show preferred azimuthal orientation in the plane on which they lie. The anisotropy of sea ice strongly influences the macromechanical behavior of first year sheet ice, while its influence on the behavior of multi-year floes, though less well studied, may be less. In first year sheet ice, the first source of anisotropy leads to a ratio of vertical to horizontal stress at constant strainrate varying from 2-5, while the second source of anisotropy leads to stress ratios of 0.25-0.60 at a 45 degree angle to the c-axis and 0.50-0.95 at a 90 degree angle.

Theoretical formulations which account for anisotropy in ice with a transversely isotropic model have been developed by Reinicke and Ralston and by Vivatrat and Chen. The former model, which assumes a generalized von-Mises yield criterion to account for pressure sensitivity and also rate independent material behavior, has been used by Ralston to predict indentation pressures based on the upper and lower bound theorems of plasticity. The results of this analysis have been incorporated in the API Bulletin 2N guidelines. The latter model, which is a pressure insensitive but rate dependent power law creep formulation, has been used to predict

indentation pressures based on the upper bound theorem.

An orthotropic elastic - power law model for sea ice has been developed assuming pressure insensitivity. This model predicts very well the plane strain uniaxial compression tests conducted by Frederking. Further, experimental data of Richter-Menge et al. on first-year sea ice and that of Hausler on saline ice indicate that sea ice is only moderately pressure sensitive in comparison with pure polycrystalline ice which is highly pressure sensitive.

A finite element method of analysis has been developed for studying the effect of sea ice anisotropy on indentation in the creeping mode. Numerical simulations of ice-structure interaction for a rigid cylindrical indenter under plane stress conditions and a tranversely isotropic version of the above material model showed that:

1. Anisotropy, as represented by the vertical stress ratio varying between 1 and 5, can cause global forces to increase by almost 15 percent depending upon whether the interface condition is fixed (infinite adfreeze bond strength), roller, or free (no adfreeze bond strength or interface friction). The factor is 1.10 for the fixed condition, 1.12 for the roller condition, and 1.13 for the free condition.
2. Anisotropy can cause maximum (peak) normal interface pressures to increase by almost 20 percent depending upon the interface condition. The factor is 1.07 for the fixed condition, 1.16 for the roller condition, and 1.19 for the free condition. The interface shear stress for the fixed condition essentially remains unchanged.
3. Finite element predictions of global forces and local pressures differ from a (approximate) modified upper bound solution by less

than about 10 percent for varying velocity, indenter diameter, and material constants.

4. Theoretical predictions of pressure area curves under "breakout" conditions provide an excellent match to measured local pressures.
5. Anisotropy leads to an increase in the size of the compression-compression and tension-tension states of stress on the upstream and downstream sides, respectively, of the indenter.
6. Anisotropy leads to decreasing strains for the roller and free conditions but to almost no change for the fixed condition. This is associated with the increase in lateral confinement near the upstream and downstream tips of the indenter which in turn significantly affects the behavior of transversely isotropic sea ice. Lateral confinement effects are smaller for the fixed condition since the influence of anisotropy is more evenly distributed over the interface due to the presence of interface shear stresses.

The numerical simulations also showed that (i) even a factor of two uncertainty in velocity will affect ice pressures only by about 20-30 percent, and (ii) the uncertainties in pressures resulting from variability in the degree of anisotropy is approximately two or three times less important than the variability of the power law constants in the reference direction. This is associated with natural variations in ice strength.

This research has been summarized in a paper entitled "Anisotropic Sea Ice Indentation in the Creeping Mode" to be presented at the Fifth International Symposium on Offshore Mechanics and Arctic Engineering, Tokyo, Japan, April 13-17, 1986 (Appendix A).

SEA ICE IDENTATION ACCOUNTING FOR FRACTURE

Field observations of sea ice identation on offshore structures in the Arctic show that fracture processes are a major factor in ice-structure interaction.

Fracture manifests itself in terms of tensile cracking and crushing in compression. Numerical simulations of ice-structure interaction processes in the creeping mode of deformation have indicated that the ice sheet consists of three regimes of principal stresses and strains; i.e., compression-compression, compression-tension, and tension-tension. The latter two regimes occupy a major fraction of the area of the continuum. Since ice is weaker in tension than in compression, accounting for the differing behavior of ice in tension may help to reduce (or limit) ice force predictions significantly.

A constitutive model for sea ice, applicable to monotonic uniaxial loading in both compression and tension, has been proposed and calibrated with experimental data. The stress-strain-strainrate behavior of sea ice has been modelled accounting for strain softening and for fracture which manifests itself in terms of tensile cracking and crushing in compression. The adequacy of the model has been demonstrated by comparison with experimental data obtained under constant strainrate, creep, and constant stressrate conditions. The model has been used to predict the occurrence of first cracks in ice under uniaxial compressive loading. Tensile strains occur under this loading condition as a result of the Poisson effect and incompressibility condition. Once cracks occur, the material continues to sustain compressive load but loses its ability to carry tensile loads in the transverse direction if applied. This is a realistic assumption and has been used often in modeling concrete behavior. A limiting tensile strain

criterion dependent on the instantaneous strainrate in tension has been used to predict crack nucleation. The results for compressive creep compare very well with the experimental data of Gold.

This research has been summarized in a paper entitled "Ductile to Brittle Transition in Sea Ice Under Uniaxial Loading" presented at the 8th International Conference on Port and Ocean Engineering under Arctic Conditions, Narssarssuaq, Greenland, September 7-14, 1985.

There are many aspects of sea ice behavior that have to be included when numerically simulating rate-dependent fracture processes. For this purpose, a rate-sensitive damage model has been developed for describing the continuum behavior of sea ice under variable loading conditions . The model, based on a nonlinear generalization of the Maxwell differential formulation, is characterized by its ability to (a) decompose the various recoverable (instantaneous elasticity and delayed elasticity or primary creep) and irrecoverable (secondary creep and strain-softening or tertiary creep) components of strain, (b) represent continuously damaging or strain softening material behavior during ductile to brittle transition in compression with a linear incremental damage accumulation model, (c) capture the rate-dependent behavior of sea ice with rate-independent model parameters, and (d) describe materially anisotropic mechanical behavior with a pressure insensitive but rate dependent potential function. Further, the model shows strong dependency of the continuum behavior under creep and constant strainrate conditions. The model predictions compare very well with several independent sets of data, particularly those for first-year sea ice. The following specific conclusions can be drawn:

1. The uniaxial model developed here is described by 8 parameters. For comparable models, i.e., those of Sinha and Michel, the number of

parameters is 7 and 9 respectively. It must be recognized that Sinha's model does not capture material damage with strain softening, while verification of Michel's model with experimental data has been very limited.

2. All parameters of the model, i.e., 8 for the uniaxial model and 5 for the orthotropic generalization, can be determined from conventional tests conducted on ice. The experimental data base is generally adequate to determine the model parameters. In particular, normalization of the uniaxial strength data for salinity and temperature is a useful way of including test results for pure polycrystalline ice in model calibration.
3. Material damage that can be described by the continuum model proposed here is significant in the strainrate range of 2×10^{-4} s^{-1} to 10^{-2} s^{-1}. At higher strainrates the presence of microcracks precludes a solely continuum description of ice behavior.
4. According to the proposed model, an ideal creep test does not lead to primary creep strains. However if the finite rise time required to reach the nominal stress in a creep test is taken into account, primary creep strains are simulated by the model. Experimental evidence appears to support this conclusion.
5. The pressure-insensitive orthotropic model proposed here predicts very well the plane strain uniaxial compression test results of Frederking. Further, experimental data of Richter-Menge et al. on first-year sea ice and that of Hausler on saline ice indicate that sea ice is only moderately pressure sensitive in comparison with pure polycrystalline ice which is highly pressure-sensitive.

This work has been summarized in a paper entitled "A Rate Sensitive

Damage Model for the Continuum Behavior of Sea Ice" in submission for publication in the Cold Regions Science and Technology Journal.

The continuum model just discussed has been unified with a second rate-sensitive model that has been developed for describing the macroscale yielding and fracture behavior of sea ice. The latter model is characterized by its ability to (a) predict first crack occurrence or nucleation with a rate-dependent limiting tensile strain criterion, and (b) represent macrocracking representing either yielding of the material or fracture depending on the stress state with a Drucker-Prager failure surface. The model predictions compare well with the limited existing experimental data base. The following specific conclusions can be drawn:

1. The prediction of first crack nucleation under uniaxial compressive creep conditions using a rate dependent limiting tensile strain criterion for the lateral tensile strains arising from Poisson's effect and incompressibility of flow compares very well with the experimental data of Gold.
2. The time to first crack occurrence tends to approah zero as the uniaxial compressive stress approaches a value corresponding to fracture, i.e., 5.0 MPa. At these higher stresses, the delayed elastic strain criterion of Sinha continues to predict longer first crack nucleation times.
3. The prediction of first crack occurrence under constant stressrate conditions using the limiting tensile strain criterion agrees very well at low to intermediate stressrates with the analysis of Sanderson and Child based on the delayed elastic strain criterion. At high stressrates, the proposed model predicts a significantly lower stress for nucleation of the crack.

4. A rate-sensitive and isotropic Drucker-Prager failure surface is used to describe yield of ice under compressive states of stress and fracture of ice whenever a tensile stress is present. The constants of the model are derived fromtwo uniaxial tests, one in tension and the other in compression. In the latter case, the compressive stress at which the first crack nucleates using the rate dependent limiting tensile strain criterion defines the "yield" point.
5. The ratio of the yield stress in uniaxial compression to the fracture stress in uniaxial tension obtained from the Drucker-Prager formulation appears to provide the best match to data from the tensile triaxial tests of Haynes.

This integrated constitutive theory for ice is able to distinguish the mechanisms of multiaxial flow as a continuum and ultimate failure by macrocracking leading to yielding of the material or fracture.

The quantification of fracture behavior requires two criteria, one for initiation and the other for propagation. Fracture initiation can often be well described by a stress or strain criterion. However, two alternative approaches are available to describe fracture propagation: a tensile limiting strain or strength criterion, and a fracture mechanics based criterion.

In the case when ice is a load bearing system, a fracture mechanics criterion for cracking is conservative. However, when ice features act as load transmitting systems, a fracture mechanics approach may lead to unconservative results. To account for tensile cracking and compressive fracture in ice and still be conservative in force and pressure predictions, a rate-dependent limiting strain or stress criterion is preferable to the fracture mechanics approach. The former is adopted in this project.

Several approaches are available to account for cracking in a finite element framework. Two of the more common approaches are the discrete cracking models which follow individual discrete cracks between elements and the smeared cracking models which treat the gross (smeared) effect of cracks in an element. The latter approach has been preferred in finite element analyses of concrete since it is computationally far more convenient, and is adopted here. An added advantage is that smeared crack models can be extended easily to allow for an objective energy release rate criterion for fracture propagation. The resulting theory, called the blunt crack band theory, will require the development of an appropriate modifica-tion to the rate-dependent limiting tensile stress fracture criterion.

A major research effort is being undertaken to (1) extend the plane stress finite element analysis computer code to incorporate smeared cracking models, and (2) implement the constitutive model in the program. The influence of fracture on both global forces and local pressure will then be quantified through numerical simulations.

3. NOTABLE NON-TECHNICAL ACTIVITIES

PUBLISHED OR SUBMITTED PAPERS

1. Ting, S-K., and Shyam Sunder,, S., "Sea Ice Indentation Accounting for Strain-Rate Variation," Proceedings of the ASCE Specialty Conference: ARCTIC '85 - Civil Engineering in the Arctic Offshore, San Francisco, CA, March 25-27, 1985, pp. 931-941.

2. Chehayeb, F.S., Ting, S-K., Shyam Sunder, S., and Connor, J.J., "Sea Ice Indentation in the Creeping Mode," Proceedings of the 17th Annual Offshore Technology Conference, Houston, TX, May 6-9, 1985, OTC Paper 5056, pp. 329-341. Paper to be simultaneously reviewed for publication in the Journal of Engineering Mechanics, ASCE.

3. Shyam Sunder, S., and Ting, S-K., "Ductile to Brittle Transition in Sea Ice Under Uniaxial Loading," Proceedings of the 8th International Conference on Port and Ocean Engineering Under Arctic Conditions, Narssarssuaq, Greenland, September 6-13, 1985.

4. Shyam Sunder, S., Ganguly, J., and Ting, S-K., "Anisotropic Sea Ice Indentation in the Creeping Mode," Proceedings of 5th International Symposium on Offshore Mechanics and Arctic Engineering, Tokyo, Japan, April 13-18, 1986. Paper to be simultaneously reviewed for publication in the Journal of Energy Resources Technology, ASME.

5. Ting, S-K., and Shyam Sunder, S., "A Rate-Sensitive Damage Model for the Continuum Behavior of Sea Ice," Cold Regions Science and Technology, In Submission, December 1985.

6. Ting, S-K., and Shyam Sunder, S., "A Rate-Sensitive Model for the Yielding and Fracture Behavior of Sea Ice," Cold Regions Science and Technology, In Submission, December 1985.

RESEARCH REPORTS

1. Ting, S-K., and Shyam Sunder, S., "Constitutive Modeling of Sea Ice with Applications to Indentation Problems," Center for Scientific Excellence in Offshore Engineering Research Report No. CSEOE 3, In Final Preparation, December 1985.

SEMINARS AND TALKS

1. Both Professors S. Shyam Sunder and Jerome J. Connor participated in the Workshop on Breaking Process of Ice Plates held at M.I.T. on November 1-2, 1984. The title of their presentations are listed below:

a. Professor S. Shyam Sunder: Sea Ice Indentation Accounting for Strain-Rate Variation.

b. Professor Jerome J. Connor: Numerical Simulation of the Creep Mode in Ice-Structure Interaction.

Professor S. Shyam Sunder was invited to talk on the same topic at the weekly seminar of the Constructed Facilities Division of the Department of Civil Engineering at MIT on December 5, 1984.

2. Professor S. Shyam Sunder was invited to talk on "Sea Ice and Its Mechanical Behavior" at a series of seminars on Engineering in the Arctic organized during MIT's Independent Activities Period, January 1985.

3. Professor S. Shyam Sunder made a presentation on this research project to the Regional Operations Technology Assessment Committee, Alaska OCS Region, of the Minerals Management Service at Anchorage, Alaska, on October 16, 1985.

PROFESSIONAL ACTIVITIES

1. Professor S. Shyam Sunder was a member of the Conference Committee for ARCTIC '85 - Civil Engineering in the Arctic Offshore Speciality Conference of the ASCE neld in San Francisco, March 25-27, 1985. He was also moderator for a session on Probabilistic Methods in Arctic Offshore Engineering.

2. Professor S. Shyam Sunder is Chairman of ASCE's Subcommittee on Arctic and Frontier Regions. This subcommittee operates under the ASCE Structural Division's Committee on Reliability of Offshore Structures. This Committee met at San Francisco in conjunction with item 3.

3. Professor S. Shyam Sunder has been appointed Vice-Chairman of the ASCE Task Committee on Reliability-Based Techniques for Designing Offshore Arctic Structures which is entrusted with the responsibility of producing

a monograph bearing the same name. He attended the Task Committee meetings at San Francisco (March 1985) and Houston (May 1985).

4. Professor S. Shyam Sunder attended the Arctic Energy Technologies Workshop organized by the U.S. Department of Energy as part of a recently initiated Arctic and Offshore Research Program. The workshop was held at Morgantown, West Virginia, on November 14-15, 1984. He also participated in the discussion group on Arctic Offshore Structures which had the task of defining the state-of-the-art, identifying technical issues, listing research and development needs, and recommending topics for research support by the U.S. DOE.

5. Professor S. Shyam Sunder participated in a workshop on "Northern Research Needs in Civil Engineering" organized by the University of Alaska, Fairbanks, in Seattle, WA, February 16-17, 1985. The workshop was sponsored by the National Science Foundation to help formulate a five year plan for Arctic research under its mandate for implementing the Arctic Research & Policy Act of 1984. Professor Shyam Sunder contributed to the Committee on Offshore and Coastal Facilities, Design and Construction.

6. Professor Jerome J. Connor is leading the organization of an International Conference on Ice Technology (ITC '96) to be held at MIT, June 10-12, 1986. An international Scientific Advisory Committee has been set up with Professor Connor and Dr. C.A. Brebbia of Southampton University, England, as Co-Chairmen. This conference will be sponsored by the Center for Scientific Excellence in Offshore Engineering at MIT, the Centre for Advanced Engineering Studies at the University of Southampton, and the MIT Sea Grant Program.

7. Professor S. Shyam Sunder attended a meeting of the Ice Mechanics Committee of ASME's Offshore Mechanics and Arctic Engineering Division of

which he is a member at Dallas, TX in February 1985.

8. Professor S. Shyam Sunder attended a meeting of ASCE's Committee on Reliability of Offshore Structures of which he is a member at Houston, TX in May 1985.

9. Professor S. Shyam Sunder has been invited to serve as a member of the Conference Committee for POAC '87, the 9th International Conference on Port and Ocean Engineering under Arctic Conditions. He is organizing technical sessions on Numerical Modeling of Ice-Structure Interaction and Probabilistic Methods in Arctic Offshore Engineering.

EXPERIMENTAL DATA FROM U.S. ARMY CRREL

An informal agreement has been reached with the U.S. Army Cold Regions Research and Engineering Laboratory, Hanover, N.H., Group under the leadership of Dr. Gordon Cox concerning our use of experimental data obtained by them. Under this agreement we can have immediate access to all their experimental data, although any publication by us of their data would in general be dated after they have had an opportunity to publish the results themselves.

HONORS AND AWARDS

Professor S. Shyam Sunder has been awarded the Gilbert W. Winslow Career Development Chair by MIT's Department of Civil Engineering for the period 1985-87. The Chair, awarded on a rotating basis to an untenured associate professor in the Department, recognizes outstanding accomplishments in teaching and research. The Chair provides unrestricted funds to Profeesor Shyam Sunder to pursue his research and teaching career at MIT. During FY 1987, the available funds equal $39,850 (note: this amount is not subject to MIT's overhead/indirect expense charges.)

4. BUDGET

The total expenditure as of November 30, 1985 is $ 59107.08. This reflects expenditures for the fifteen month period September 1, 1984 (the requested project starting date) through the end of November.

Professor S. Shyam Sunder is charging 20% of his salary to the MMS and SOHIO accounts respectively since September 1, 1985. Mr. S-K Ting was a full-time Research Assistant on the project from September 1, 1985 through October 31, 1985; the day he submitted his doctoral thesis at MIT and left to join the faculty at the National University of Singapore. Mr. J. Ganguly was a full-time Research Assistant from September 1, 1985 through January 15, 1985. During the Fall-Term these salaries were charged to the SOHIO account. Mr. Chia-Wey Chen, a doctoral student with considerable expertise in computational mechanics and work experience in the nuclear power industry, will be joining the project as a full-time Research Assistant on January 1, 1985.

ANISOTROPIC SEA ICE INDENTATION IN THE CREEPING MODE

by

S. Shyam Sunder
Winslow Associate Professor of Civil Engineering

and

Jaideep Ganguly and Seng-Kiong Ting
Research Assistants, Department of Civil Engineering
Massachusetts Institute of Technology
Cambridge, Massachusetts 02139

ABSTRACT

An orthotropic elastic - power law creep model for sea ice is presented and then a finite element method of analysis is developed and applied to study the effect of sea ice anisotropy on indentation in the creeping mode. Numerical simulations are performed under plane stress conditions to predict the influence of interface adfreeze and friction, variability in parameters of a transversely isotropic material model for sea ice, rubble pile or grounded ice foot, and ice sheet velocity on global forces and local pressures generated on a rigid cylindrical indenter. The results are compared with those from an approximate methods of analysis based on the upper bound theorem. Interface pressure distributions are obtained in addition to contours of stress and strain.

INTRODUCTION

The interaction of an ice sheet with a vertically faced indenter is an important loading condition for cylindrical structures and conical structures with grounded rubble pile or accreted ice foot in the Arctic. In general, this indentation phenomenon is characterized by the simultaneous occurrence of viscous (rate-dependent) and fracture behavior.

Several theoretical models based on approximate methods of analysis that idealize the ice sheet as an isotropic continuum have been proposed for predicting global ice forces. These include: (1) the upper and lower bound, plasticity solutions of Michel and Toussaint (1) based on the Von-Mises yield criterion, and Croasdale et al. (2) based on the Tresca yield criterion, (2) the reference stress, power law creep solution of Ponter et al. (3), and (3) the upper bound, power law creep solutions of Bruen, Vivatrat and Chen (4,5), and Ting and Shyam Sunder (6). Theoretical predictions of interface pressures are not generally available. However, Ting and Shyam Sunder (6) have applied the (approximate) strain path method of analysis to study interface pressures during plane strain indentation. Their study showed that approximate methods of analysis cannot adequately model interface adfreeze and friction, factors that can significantly influence ice load predictions. In a recent paper (7), two of the authors and their colleagues have developed and applied a finite element ("exact") method of analysis to predict both global forces and local pressures assuming an isotropic elastic - power law creep model for sea ice.

Sea ice, however, is not an isotropic material. Field observations have shown that this type of ice, which is predominantly columnar, has two sources of anisotropy: (a) the c-axis is oriented perpendicular to the axis of crystal growth, and (b) the c-axes of different crystals may show preferred azimuthal orientation in the plane on which they lie. There is strong evidence suggesting that the preferred azimuthal orientation is correlated with the instantaneous current direction just underneath a growing ice sheet (8,9,10). While such alignments are common in landfast ice, observations suggest that strong alignments can develop in pack ice when there is little rotation of the floes relative to the current direction (11,12).

The anisotropy of sea ice strongly influences the macromechanical behavior of first year sheet ice, while its influence on the behavior of multi-year floes, though less well studied, may be less. In first year sheet ice, the first source of anisotropy leads to a ratio of vertical to horizontal stress at constant strainrate varying from 2-5 (13-17), while the second source of anisotropy leads to stress ratios of 0.25-0.60 at a 45 degree azimuthal angle to the c-axis and 0.50-0.95 at a 90 degree angle (18-21).

Theoretical formulations which account for anisotropy in ice with a transversely isotropic model have been developed by Reinicke and Ralston (22) and by Vivatrat and Chen (23). The former model, which assumes a generalized Von-Mises yield criterion to account for pressure sensitivity and also rate

independent material behavior, has been used by Ralston (24) to predict indentation pressures based on the upper and lower bound theorems of plasticity. The results of this analysis have been incorporated in the API Bulletin 2N guidelines (25). The latter model, which is a pressure insensitive but rate dependent power law creep formulation, has been used to predict indentation pressures based on the upper bound theorem.

A study of sea ice indentation in the creeping mode is important for two reasons: (a) creep is the predominant mode of deformation for artificial islands in the Arctic nearshore region during "breakout" and/or steady indentation conditions occuring during the winter, and (b) stresses, strains, and strainrates resulting from creep are necessary to predict the nucleation, growth initiation and propagation of cracks when viscous effects influence fracture behavior. The latter scenario, which defines the transition from ductile to brittle behavior, may represent the most severe loading case since indentation pressures tend to be lower at very fast ice movement rates. It may be noted that at very high rates of loading ice behaves essentially as a brittle elastic material.

This paper is concerned with (i) the development of an orthotropic elastic - power law creep model for sea ice, and (ii) the development and application of a finite element method of analysis to study the influence of sea ice anisotropy on indentation in the creeping mode. Numerical simulations are performed under plane stress conditions to predict the influence of interface adfreeze and friction, variability in material constants for a transversely isotropic model of sea ice, rubble pile or accreted ice foot, and ice sheet velocity on global forces and local pressures generated on a rigid cylindrical indenter. The results are compared with those from an approximate method of analysis based on the upper bound theorem. Interface pressure distributions are obtained in addition to contours of stress and strain.

MATERIAL MODELING

Theoretical Formulation

The rate-dependent material model for sea ice assumes that the total strainrate is the sum of the elastic strainrate and the creep or viscous strainrate, i.e.,

$$\dot{\underline{\varepsilon}} = \underline{C}\,\dot{\underline{\sigma}} + \dot{\underline{\varepsilon}}_c \tag{1}$$

where $\underline{C}$ is the linear elastic compliance matrix for an orthotropic material.

To derive the relationship between the creep strainrate and stress vectors, first an effective stress measure generalized for pressure insensitive orthotropic materials, i.e., identical behavior in compression and tension, is defined.

$$\sigma_e^2 = 3/A\left[\frac{a_1}{3}(\sigma_{xx}-\sigma_{yy})^2 + \frac{a_2}{3}(\sigma_{yy}-\sigma_{zz})^2 + \frac{a_3}{3}(\sigma_{zz}-\sigma_{xx})^2 + 2a_4\,\sigma_{xy}^2 + 2a_5\,\sigma_{yz}^2 + 2a_6\,\sigma_{zx}^2\right] \tag{2}$$

with $A=a_1+a_2$. This may be expressed in compact form using matrix notation as:

$$\sigma_e^2 = 3/A\;\underline{\sigma}^T\,\underline{G}\,\underline{\sigma} \tag{3}$$

Under uniaxial (compressive) loading conditions, creep in ice is usually expressed in terms of a power law (26). Then, the effective strainrate and effective stress are related by:

$$\dot{\varepsilon}_e = a\,\sigma_e^N \tag{4}$$

where the effective strainrate can be expressed in terms of the creep strainrate vector as given in Refs. (27, 28), a and N are constants with the temperature dependence being included in the parameter a following an Arrhenius activation energy law. Mellor (29) states that for temperatures greater than -10°C the law is not valid and that the complete empirical relation derived from experiments should be used to model temperature dependence in such cases.

The strainrate vector can be related to the effective stress vector by defining a scalar potential function ϕ which obeys the associated flow rule, i.e.,

$$\dot{\underline{\varepsilon}}_c = \frac{\partial \phi}{\partial \underline{\sigma}} \tag{5}$$

with

$$\phi = a\,\frac{\sigma_e^{N+1}}{N+1} \tag{6}$$

Combining Eqs. (5), (6) and (3) yields the desired relationship:

$$\dot{\underline{\varepsilon}}_c = \lambda\,\underline{S}^* \tag{7}$$

where

$$\lambda = 3/A\;a\;\sigma_e^{N-1} \tag{8}$$

and

$$\underline{S}^* = \underline{G}\,\underline{\sigma} \tag{9}$$

Note that $\underline{S}^*$ is not the conventional deviatoric stress vector. It may be thought of as a pseudo deviatoric stress vector for an anisotropic material.

Given the stress vector, the pseudo deviatoric stresses may be obtained from Eq. (9). Then applying Eqs. (3), (8), and (7) in succession leads to the creep strainrate vector. Note that under isotropic conditions, i.e., $a_1 - a_6 = 1$, all these equations reduce to the formulation proposed by Palmer (30) and described in Ref. (7).

Estimation of Model Parameters

Six uniaxial (compression) tests at constant strainrate are necessary to obtain the seven orthotropic model parameters: a, N, a_2-a_6. Note that (i) a_1 can be set equal to one without loss of generality, and (ii) there is experimental evidence which shows that the power law exponent N can be considered independent of the direction of loading. For purposes of the current derivation, it is assumed that the x-axis is normal to the ice sheet and that y-z defines the horizontal plane of the ice sheet. Furthermore, it is assumed that the c-axes of the sea ice crystals lie on the y-z plane and that they are

aligned in the y-direction. This implies that the x-axis represents the crystal growth direction.

Let the tests be conducted in the three orthogonal directions y, x and z respectively, and along the three 45° axes on the y-z, x-y and z-x planes respectively. Furthermore, let β_1-β_5 represent the experimentally determined ratios of the maximum stresses for the last five tests, respectively, to the maximum stress in the reference y-direction at the same strainrate. According to the theoretical formulation, the parameters a and N refer directly to the uniaxial test along the c-axis, i.e., the y-direction. The remaining parameters may be determined from the following equations:

$$a_2 = -\frac{\beta_1^n - \beta_2^n(1-\beta_1^n)}{\beta_1^n - \beta_2^n(1+\beta_1^n)} \tag{10}$$

$$a_3 = -\frac{\beta_1^n + \beta_2^n(1-\beta_1^n)}{\beta_1^n - \beta_2^n(1+\beta_1^n)} \tag{11}$$

$$a_4 = \frac{A}{6}\left[4\beta_4^{-n} - \beta_2^{-n}\right] \tag{12}$$

$$a_5 = \frac{A}{6}\left[4\beta_3^{-n} - \beta_1^{-n}\right] \tag{13}$$

$$a_6 = \frac{A}{6}\left[4\beta_5^{-n} - 1\right] \tag{14}$$

where n=2N/(N+1). Typical ranges for the βi's are 2-5 for β_1 (13-17), and 0.50-0.95 and 0.25-0.60 respectively for β_2 and β_3 (18-21). Values for β_4 and β_5 are not generally available in the literature. Since these two parameters determine only the out of plane shear strains and stresses in sheet ice, they have no influence on plane strain and plane stress indentation problems. However, the parameters will have to be obtained in the case of three-dimensional indentation problems.

For a tranversely isotropic material, i.e., isotropy in the y-z plane, $\beta_2=\beta_3=1$ and $\beta_4=\beta_5$. As a result $a_1=a_3=1$, $a_4=a_6$, the parameters a_2 and a_5 are functions of only β_1, while a_4 depends on both β_1 and β_4. Only three uniaxial tests are required to obtain a, N, β_1 and β_4; one each in the y and x directions and one along the 45° axis on the x-y or z-x planes.

Frederking (31) has conducted plane strain uniaxial compression tests on columnar-grained transversely isotropic freshwater ice. For his type A tests, strains in the z-direction are constrained to zero and stresses are applied in the y-direction. The ratio Γ_z of the plane strain stress to the unconfined stress at the same strainrate is directly related to β_1 by the following equation:

$$\Gamma_z = \left[\frac{4\beta_1^{2n}}{4\beta_1^n - 1}\right]^{1/n} \tag{15}$$

The equation predicts Γ_z to vary between 2.1-5.1 for experimentally observed values of β_1 ranging from 2 to 5, and N between 3 and 4. This is consistent with Frederking's experimental observations of Γ_z which were close to 2 at high strainrates and to 5 at low strainrates. In the type B tests, strains in the x-direction are constrained to zero while stresses are again applied in the y-direction. In this case, the stress ratio Γ_x is given by:

$$\Gamma_x = \left[1 + \frac{1}{4\beta_1^n - 1}\right]^{1/n} \tag{16}$$

Since β_1 is generally greater than one, Γ_x will be less than approximately 1.2 for N between 3 and 4. For typical values of β_1, the predicted values of Γ_x range from 1.01 to 1.06. This is consistent with Frederking's experiments which showed negligible influence of x-direction confinement on stresses.

Triaxial tests of first-year sea ice have been conducted by Richter-Menge, Cox et al. (20) on samples obtained from horizontal cores in the plane of the ice sheet at angles of 0°, 90°, and 45° to the preferred c-axis orientation. According to the orthotropic material model, the ratio Γ_t of the maximum axial stress with a confining pressure equal to τ times the axial stress to the maximum axial stress in the unconfined state at the same strainrate should be given by:

$$\Gamma_t = \frac{1}{1-\tau} \tag{17}$$

The shear stress (i.e., axial stress minus radial stress) normalized by the unconfined stress is independent of τ or confining pressure for the model and equal to one. Experimental data for this quantity is plotted versus confining pressure in Fig. 1, which shows that the sea ice data is only moderately pressure sensitive. Thus the use of a pressure insensitive model may be justified for sea ice, particularly when other sources of uncertainty such as the variablity in the power law constant a are considered. The figure also includes data obtained by Hausler (32) on columnar-grained saline ice at a strainrate of 2×10^{-4} s^{-1} using a so-called "true" triaxial testing machine.

The experimental results of Panov and Fokeev (33) for natural and artificial sea ice, however, seem to indicate an appreciable increase in shear stress with confining pressure. Their tests were carried to the "breaking point" and as a consequence that data cannot be used to characterize the flow behavior of ice. On the other hand, the triaxial behavior of pure (non-saline) polycrystalline ice has been studied by Jones (34, 35). The tests performed at strainrates of 10^{-6} to 5×10^{-3} s^{-1} indicate up to a factor of two increase in shear stress due to confining pressure. This data for pure ice has limited applicability for calibration of sea ice models since no equivalence in the triaxial behavior of pure and sea (saline) ice has been established. It must be noted that the plasticity based pressure sensitive parabolic yield function of Reinicke and Ralston (22) has been justified with the help of Frederking's (31) data (which has been shown in this paper to follow a pressure insensitive model very well) and that the three parameter but isotropic extension of their yield function by Reinicke and Remer (36) has been justified on the basis of Jones's triaxial data for pure polycrystalline ice.

FINITE ELEMENT SIMULATIONS

Theoretical Formulation

For general viscoplastic behavior, which includes creep, it is convenient to work with time derivatives of the governing equations for a solid. The weighted equilibrium-rate equation which forms the basis of the finite element displacement method is then given by:

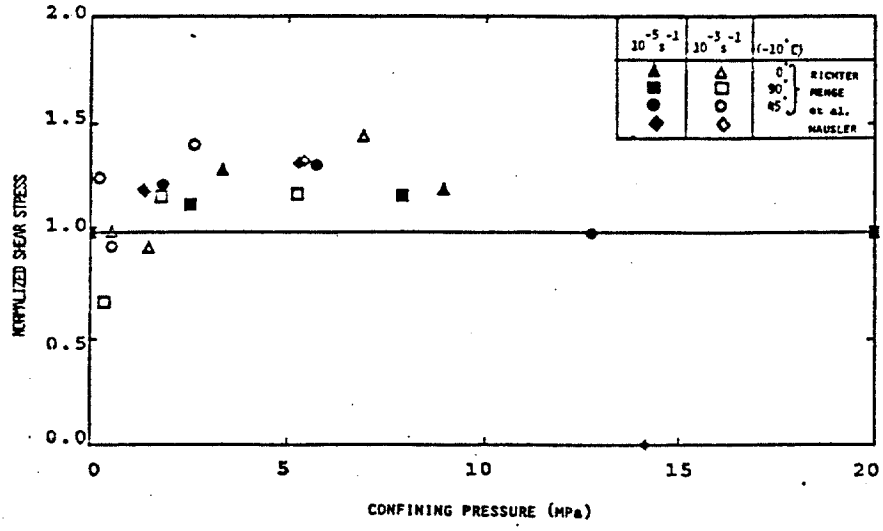

Fig. 1 - Normalized Shear Stress Versus Confining Pressure

$$\int \underline{B}^T \dot{\underline{\sigma}}\, dV = \dot{\underline{P}} \tag{18}$$

where $\underline{B}$ is the strainrate - nodal velocity transformation matrix derived from the chosen displacement expansion for the finite element, i.e.,

$$\dot{\underline{\varepsilon}} = \underline{B}\,\dot{\underline{U}} \tag{19}$$

and $\dot{\underline{P}}$ is a vector defining the applied rate of loading, if any, at the nodes of the finite element. Examples include driving forces such as wind and current shear. Equation (18) may also be derived from the virtual work principle. Combining Eqs. (18) and (19) with Eq. (1) and defining $\underline{K}=\underline{B}^T\underline{D}\underline{B}$ as the elastic stiffness matrix of the element leads to the element equilibrium equation:

$$\underline{K}\,\dot{\underline{U}} = \dot{\underline{P}} + \int \underline{B}^T \underline{D}\,\dot{\underline{\varepsilon}}_c\, dV \tag{20}$$

and the element stressrate - nodal velocity relations:

$$\dot{\underline{\sigma}} = \underline{D}\,\underline{B}\,\dot{\underline{U}} - \underline{D}\,\dot{\underline{\varepsilon}}_c \tag{21}$$

where $\underline{D}$ is the linear elastic rigidity matrix for an orthotropic material. The global stiffness matrix $\underline{K}_G$ is obtained from Eq. (20) using conventional procedures. This formulation can take into account the spatial and temporal variability of the strainrate field in the ice sheet.

An iterative solution algorithm has been developed to solve the pseudo-force form of the nonlinear governing equations given in Eqs. (20) and (21). This is a generalization of the algorithm for isotropic materials presented in an earlier paper (7) and is fully discussed in Refs. (27,28). The conceptual basis for the algorithm may be illustrated by focussing attention at the element level rather than the global level. At first the governing equations are integrated in time between t_i and t_{i+1} to yield:

$$\underline{K}(\underline{U}_{i+1}-\underline{U}_i)=\underline{P}_{i+1}-\underline{P}_i+\int \underline{B}^T\underline{D}(\underline{\varepsilon}_{c,i+1}-\underline{\varepsilon}_{c,i})\,dV \tag{22}$$

$$\underline{\sigma}_{i+i}-\underline{\sigma}_i=\underline{D}\underline{B}\underline{U}_{i+1}-\underline{U}_i)-\underline{D}(\underline{\varepsilon}_{c,i+1}-\underline{\varepsilon}_{c,i}) \tag{23}$$

Creep strains which appear in both equations are nonlinear functions of stress since λ in Eq. (7) is not a constant. A two-level iterative algorithm is used to solve these equations for each new time step t_{i+1}. The key steps in the solution algorithm are as follows:

1. Compute the displacement increments from (the global form of) Eq. (22) for the given loading vector. In the first iteration on the equation, the incremental creep strains are assumed to be zero.
2. Compute the incremental stresses and incremental creep strains from Eq. (23) for the displacement increments obtained in step 1 using the lower-level iterative algorithm discussed below. In the first iteration on this equation assume the incremental creep strains to be zero.
3. Return to step 1 and iterate on Eq. (22) (higher-level iteration) using the incremental creep strains obtained in step 2 until convergence is achieved. The evaluation of the integral defining the inelastic load vector is based on a Gaussian quadrature formula. Typically, 4-6 iterations are required for convergence at the higher level.

The evaluation of the incremental stresses and incremental creep strains in step 2 requires the simultaneous consideration of Eq. (23) and Eq. (7). In addition to a nonlinear equation solver, a numerical time integrator is needed to obtain results. For accelerating solution convergence in creep dominant problems with negligible elastic deformations that are of concern here, a lower-level algorithm is developed which combines a Newton-Raphson or tangent type nonlinear equation solver with the α-method of numerical time integration. Details of the solution algorithm may be found in Refs. (27,28). Application of the lower-level iteration with $\alpha=1$, which yields an implicit algorithm, shows that convergence is typically obtained in 4 iterations.

Description of Numerical Simulations

Numerical simulations are performed for the 13 cases identified in Table 1 based on a transversely

isotropic elastic - power law creep material model for sea ice.

The objectives of simulations 1-3 and 9-13 are to quantify the effect of interface adfreeze and friction on predicted indentation pressures. For global forces, the fixed condition provides an upper bound solution since the ice-structure interface is considered to be infinitely strong. In this case, the nodes of the finite element mesh (see Fig. 2) at the ice-structure interface are constrained from moving in any direction. The free condition corresponds to no adfreeze and friction, while the roller condition provides an intermediate solution. The roller condition allows no normal motion of the finite element nodes at the ice-structure interface but tangential motion at the interface is not constrained. On the other hand, the free condition allows only normal compressive stresses to develop at the ice-structure interface. Thus the upstream side tends to follow the roller condition and may be modelled as such. However, the interface nodes of the ice and the structure are completely disconnected if a normal tensile stress develops. This is an adaptive process in general, but for the numerical simulations considered in this paper it was found adequate to disconnect the downstream interface nodes to achieve the desired no-tension condition.

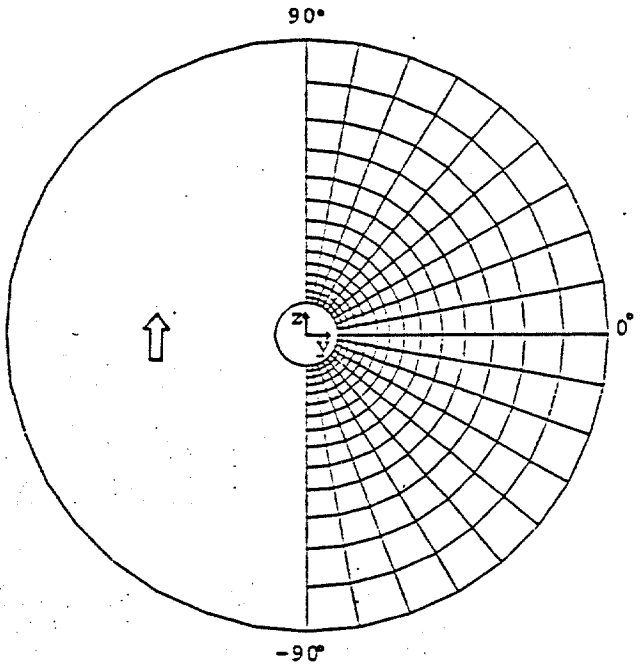

Fig. 2 - Finite Element Grid

Simulations 4 and 5 study the influence of ice sheet velocity on pressures. The chosen base velocity of 0.195 m/hr corresponds to the recorded maximum average velocity over a twelve-hour period just prior to "breakout" (macrocracking) for an artificial island in the Beaufort Sea. This is selected in order to predict the maximum ice presssure on the structure which is assumed to occur just prior to macrocrack formation or "breakout" where ice deforms primarily in the creeping mode. Macrocracks tend to relieve the stresses built up in the ice sheet and as such reduce ice pressures. The sixth simulation attempts to quantify the effect of a grounded rubble pile or an accreted ice foot on ice pressures by defining a larger effective indenter diameter (2.85 times the structural diameter). The seventh simulation is used to check the construction of the pressure-area curve for large contact areas. Simulations 8-13 study the effect of variability in constants a, N, and β_1 defining the material model on ice pressures. Two sets of the parameters a and N for sea ice based on the work of Sanderson (37) and Wang (38), respectively, are considered: N=3, $a=2.125\times10^{-6}$ $(MPa)^{-3}s^{-1}$; and N=4, $a=1.848\times10^{-6}$ $(MPa)^{-4}s^{-1}$. These two sets of constants define the rate-dependent uniaxial strength of ice in the horizontal plane of the ice sheet. Three values of β_1 equal to 2,3 and 5 are studied. These define the relative values of the uniaxial strength in the directions normal to and in the horizontal plane of the ice sheet. The elastic constants in the horizontal plane of isotropy, which have negligible influence on the steady state solutions under constant strainrate conditions, are taken to be E=9.5 GPa and ν=0.3.

The criteria governing the choice of finite element mesh and time increments for the simulations are described in an earlier paper (7). The chosen uniform far-field velocity listed in Table 1 defines the excitation here. For a given time step, the excitation is specified in terms of an imposed displacement in the z-direction at the far-field boundary nodes (Fig. 2). This displacement value is made to increase linearly in time, consistent with the chosen uniform velocity.

DISCUSSION OF RESULTS

Global Forces

Table 2 lists the global pressures predicted by the finite element analysis for the 13 cases of interest. Pressure values are the global forces divided by the indenter diameter D, and ice sheet thickness t. The table also lists the factor by which the global pressure increases as a result of anisotropy.

Comparing the global pressures for cases 1-3 and 9-13, it is seen that the fixed condition does provide an upper bound solution. The global pressure for the fixed condition is greater than that for the roller condition by a factor of about 1.22 to 1.27. In turn, the global pressure for the roller condition is 1.97 to 2.00 times that for the free condition. This spread in global pressures is indicative of the influence of interface adfreeze bond and friction. The hundred percent reduction in pressure between the roller and free cases occurs because the lack of downstream interface contact in the latter case tends to release the downstream stresses in the ice sheet.

The fourth and fifth values of global pressure indicate that reducing the ice sheet velocity by a factor of 6.4 leads to a 47-48% reduction in pressures while increasing the velocity by a factor of 1.6 leads to a 15-18% increase in pressures. Thus even a factor of two uncertainty in velocity will affect the pressures only by about 20-30%.

Cases 2 and 6 provide some idea of the effect of a grounded rubble pile or an accreted ice foot. The global force increases by a factor of 1.92 when the effective indenter diameter is taken to be a multiple (2.85) of the structural diameter. In the case of a grounded rubble pile, it would be overconservative to consider that all this force is transmitted to the

TABLE 1 - SUMMARY OF CASES

Case	Velocity (ft/hr)	Diameter (ft)	N	β_1	Interface Condition
1	0.64	350	3	3	Fixed
2	0.64	350	3	3	Roller
3	0.64	350	3	3	Free
4	0.10	350	3	3	Roller
5	1.00	350	3	3	Roller
6	0.64	1000	3	3	Roller
7	0.64	328000	3	5	Free
8	0.64	350	4	3	Roller
9	0.64	350	3	5	Fixed
10	0.64	350	3	5	Roller
11	0.64	350	3	5	Free
12	0.64	350	3	2	Fixed
13	0.64	350	3	2	Free

Note: 1 ft = 0.3048 m
$a=2.125\times10^{-6}$ (MPa)$^{-N_s-1}$ for N=3; $a=1.848\times10^{-6}$ (MPa)$^{-N_s-1}$ for N=4

TABLE 2 - SUMMARY OF RESULTS

Case	P/Dt (MPa)		Maximum Interface Normal Stress (MPa)		Anisotropy/Isotropy	
	Finite Element Analysis	Modified Upper Bound	Finite Element Analysis	Modified Upper Bound	Global Pressure	Maximum Interface Normal Stress
1	2.41	2.62	0.87	0.95	1.08	1.06
2	1.98	2.06	1.10	1.15	1.12	1.12
3	0.99	1.03	1.13	1.17	1.11	1.15
4	1.03	1.11	0.58	0.62	1.10	1.12
5	2.33	2.39	1.29	1.34	1.15	1.15
6	1.33	1.45	0.74	0.81	1.08	1.09
7	0.10	0.11	0.11	0.12	-	-
8	2.57	2.43	1.43	1.36	1.22	1.25
9	2.46	2.71	0.88	0.98	1.10	1.07
10	1.99	2.13	1.14	1.19	1.12	1.16
11	1.01	1.07	1.17	1.22	1.13	1.19
12	2.35	2.49	0.85	0.90	1.05	1.04
13	0.96	0.98	1.12	1.12	1.08	1.12

Note: The maximum interface shear stress for the fixed condition is 0.61 MPa for β_1=3, 0.63 MPa for β_1=5, and 0.60 MPa for β_1=2.
1 MPa = 145 psi

foundation by the structure. On the other hand, the force transmitted to the foundation by the structure would decrease by a factor of 4.25 if both the structure and the grounded rubble pile could transmit a force proportional to the contact area of each with the foundation. These results for a transversely isotropic material are identical to that from the isotropic analysis in Ref. (7), although the absolute value of the global force for the anisotropic case is greater than that for the isotropic case by a factor of 1.08 to 1.12.

Case 8 shows that for β_1 equal to 1 (isotropic) and 3, the two sets of values for the material constants a and N lead to ice pressures for the roller condition which differ by a factor of 1.19 and 1.30, respectively. However for N=3 and the corresponding a, and β_1 varying between 1 and 5 (cases 1-3 and 9-13), global ice pressures vary by a factor of 1.10, 1.12, and 1.13 for the fixed, roller and free conditions, respectively. This indicates that the degree of anisotropy β_1 is approximately two to three times less important than the actual values of a and N.

Calibration With Approximate Solutions

In order to provide perspective and calibration with solutions based on approximate methods of

analysis, an upper bound solution corresponding to the two-dimensional velocity field postulated in Ref. (6) is obtained for a transversely isotropic power law material. The kinematic model, obtained by superposing a uniform flow and a doublet, resembles the flow of an infinite ice sheet past a circular indenter with the interface matching most the roller condition. The approximate formula may be expressed as given below:

$$\frac{P}{Dt} = \theta(\beta_1)\,\Gamma_p(\beta_1)\,\frac{4\pi}{\sqrt{3}}\,\frac{N}{N+3}\left[\frac{4}{\sqrt{3}}\cdot\frac{1}{a}\,\frac{2V}{D}\right]^{1/N} \qquad (24)$$

where P is the global force, V is the ice sheet velocity, and Γ_p is the theoretically obtained ratio of global pressures for the anisotropic and isotropic cases which is a function of only β_1, i.e.,

$$\Gamma_p = \frac{\beta_1}{\left[(4\beta_1^n-1)/3\right]^{1/n}} \qquad (25)$$

Note that $\Gamma_p=1$ under isotropic conditions, i.e., $\beta_1=1$, and that $\Gamma_p=(3/4)^{1/n}$ as $\beta_1\to\infty$. For $2.5<N<4$, this asymptotic value varies between 0.818-0.835. A fraction equal to 98.5% of the asymptotic value is reached at $\beta_1=5$. The factor θ is used to modify the upper bound solution, which corresponds to a plane strain condition as a result of the two-dimensional kinematic field selected, in order to be able to apply it under plane stress conditions. As discussed in Ref. (7), Ponter et al.'s (3) analysis for both plane strain and plane stress yields $\theta=0.5$ for the isotropic case. On the other hand as $\beta_1\to\infty$, i.e., the material becomes infinitely strong transverse to the plane of isotropy, the difference between the plane strain and plane stress conditions disappears. Thus, the ratio of the global pressures at these two extremes of anisotropy is equal to $\theta_\infty(3/4)^{1/n}/0.5$, which for N=3 is $1.65\theta_\infty$ and for N=4 is $1.67\theta_\infty$. Table 2 shows that case 11 with N=3 and $\beta_1=5$ predicts the ratio of global pressures to be 1.124 which suggests that $\theta_\infty=0.69$. This result was verified by additional simulations with β_1 equal to 10 and 20 respectively. The variation of θ with β_1 may be expressed as:

$$\theta = 0.69 - 0.19\exp[-0.7(\beta_1-1)] \qquad (26)$$

Table 2 shows that the predictions based on Eqs. (24)-(26) differ from the finite element solutions by less than 10%. The fixed condition is obtained by multiplying Eq. (24) by 1.27, while the free condition uses a multiplying factor of 0.5 (Table 3).

Local Pressures

The maximum (peak) interface normal stress for each of the 13 simulations is listed in Table 2. The table also lists the maximum interface shear stress for the fixed cases. Notice that in all cases the maximum normal pressure is approximately 0.36-1.16 times the global pressure.

The maximum normal stress for the fixed condition is lower than that for the roller condition by 16-23%, although a reverse trend is observed for global pressures. This occurs because part of the force in the fixed condition is carried by interface shear stress. On the other hand, the maximum normal stress for the free condition is about 0-3% higher than that for the roller condition. This negligible increase occurs since the small level of stresses that exist in the predominantly rigid continuum on the downstream side for the free condition is transmitted to the structure from the upstream side. These results confirm the conclusion reached in Ref. (7) that for local pressures the use of the free condition is conservative while for global forces the fixed condition is conservative.

Comparison of the local and global pressures shows that the ratio of the maximum normal interface stress to the global pressure is approximately 0.36 for the fixed condition, 0.56 for the roller condition, and 1.14 for the free condition. Furthermore, the variation of local pressures with V, D, a and N is similar to that for global pressures. Thus multiplication of Eq. (24) by 0.46, 0.56 and 0.57 can be used to estimate the respective maximum normal pressures (Table 3). In a similar fashion, the maximum interface shear stress for the fixed condition may be estimated from the equation with a multiplication factor of 0.33.

TABLE 3 - MULTIPLYING FACTORS FOR APPROXIMATE MODEL (Eq. 30)

Condition	Global Pressures	Maximum Interface Normal Stress
Roller	1.00	0.56
Fixed	1.27	0.46
Free	0.50	0.57

Note: Factor for Maximum Interface Shear Stress in Fixed Condition = 0.33

For purposes of design it is necessary to consider not only the maximum values of normal stress but also its distribution on the structure. Figure 3 presents typical normal stress distributions corresponding to $\beta_1=5$, which are very similar to the stress distributions for the isotropic case given in Ref. (7). The distributions are not affected, at least visually, as V, D, N and β_1 are varied, although they have to be scaled according to the maximum normal stresses in Table 2. A conservative design approach may be to assume a uniform or rectangular distribution of stress based on the maximum normal interface stress.

Comparison With Pressure-Area Curves

Pressure-area curves are often constructed to help designers obtain the average pressures over tributary loaded areas for structural components (see for example Ref. (39). A typical curve developed by Sanderson (40) and discussed in Ref. (7) is shown in Fig. 4. The darkly shaded areas represent field and laboratory experimental data, while the lightly shaded areas represent his extrapolation of the measurements. The dark region in the extreme left is from laboratory indentation tests, the central region reflects measurements from ice breakers traveling in the Arctic, while the two smaller regions on the right correspond to average global pressures on artificial islands estimated from pressure sensor measurements in the ice sheet. The contact area is defined as the indenter area of contact for the laboratory and artificial island data. For the ice breaker data, the contact area is the local area over which the pressure measurement is made and not the form area of the ice breaker.

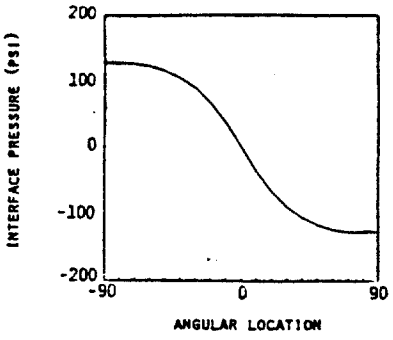

(a) Fixed Case

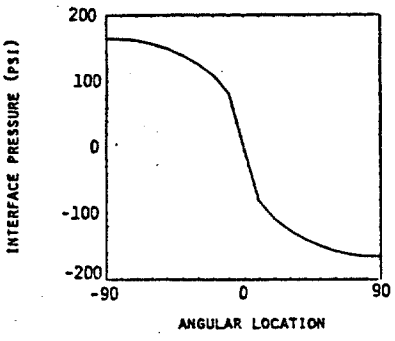

(b) Roller Case

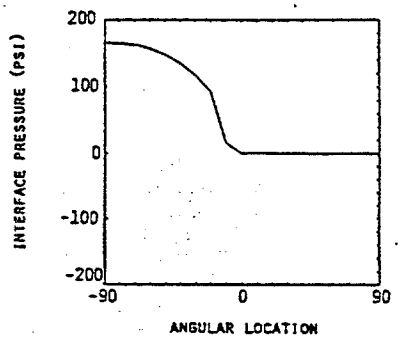

(c) Free Case

Fig. 3 - Normal Stress Distribution on Interface at Steady State for $\beta_1 = 5$

The lower solid line in Fig. 4 is the maximum normal interface stress on the indenter (defined here as the local pressure or indentation pressure) under free interface conditions predicted by Eq. (24) assuming isotropy and N=3. The contact area is taken as Dt and the ice sheet velocity is taken as 0.195 m/hr, i.e., the value just prior to "breakout". The upper solid line corresponds to an extreme level of anisotropy, i.e., β_1=5. For contact areas greater than 10 m^2 where plane stress conditions exist, the two lines differ by only a factor of 1.2. When the effective strainrate, i.e., $8/\sqrt{3}$ V/D, exceeds 5×10^{-4} s^{-1}, ice is assumed to have fractured (crushed) and the uniaxial strength is capped at 5.9 MPa, leading to the flat portion of the curve on the extreme left. These predictions represent an excellent upper bound match to measured local or indentation pressures. Thus, a more appealing interpretation of the figure is to consider the contact area as the indenter area (Dt in this paper) and not the tributary loaded area for a structural component, and the indenter pressure corresponding to a given contact area as the maximum normal interface pressure for that indenter. The distribution of the interface stresses may be assumed uniform over the indenter area of area as concluded earlier. However, a different boundary value problem (e.g., other than "breakout") involving a smaller contact area, as opposed to contact over half the perimeter in the free condition, could lead to higher interface pressures.

The theoretical predictions made here assume knowledge of the ice sheet velocity just prior to "breakout" or macrocracking. At higher velocities, fracture in ice will be the key mechanism that limits the pressures.

Multiaxial Behavior of Ice Sheet

Stress contours identifying the compression-compression, compression-tension, and tension-tension regions in the ice sheet are generally similar for both the isotropic and anisotropic material models, i.e., (a) tensile stresses occur almost all over the ice sheet, (b) the compression-compression region on the upstream side, is much smaller for the free condition than for the fixed condition, and (c) under free interface conditions the relatively small downstream stresses are predominantly tension-tension. Figures 5 and 6 show that increasing anisotropy, i.e., β_1, leads to increasing compression-compression and tension-tension regions. Experimental evidence for compression-tension states of stress (41) shows that the occurrence of even small tensile stresses weakens ice considerably, leading to premature fracture when compared with uniaxial tensile loading.

The strain fields also are very similar for isotropic and anisotropic material behavior. The strains are smaller as β_1 increases for the roller and free conditions but remain almost unchanged for the fixed condition. The reduction in strains is associated with the increase in lateral confinement near the upstream and downstream tips of the indenter which in turn significantly affects the behavior of transversely isotropic sea ice. Lateral confinement effects are smaller for the fixed condition since the influence of anisotropy is more evenly distributed over the interface due to the presence of interface shear stresses. The peak values of these stresses occur not at the tips but at points tangential to the direction of the ice movement. The strains are compression-tension almost everywhere on the ice sheet with tensile strains exceeding 0.001 at steady state. Since tensile failure strain for sea ice is about 0.001 or less for strainrates greater than 10^{-7} s^{-1} under just uniaxial loading, it seems likely that cracking will occur even before steady state is reached.

CONCLUSIONS

This paper has (i) presented an orthotropic elastic - power law creep model for sea ice, and (ii) developed and applied a finite element method of analysis to study the effect of sea ice anisotropy on indentation in the creeping mode. A pressure-

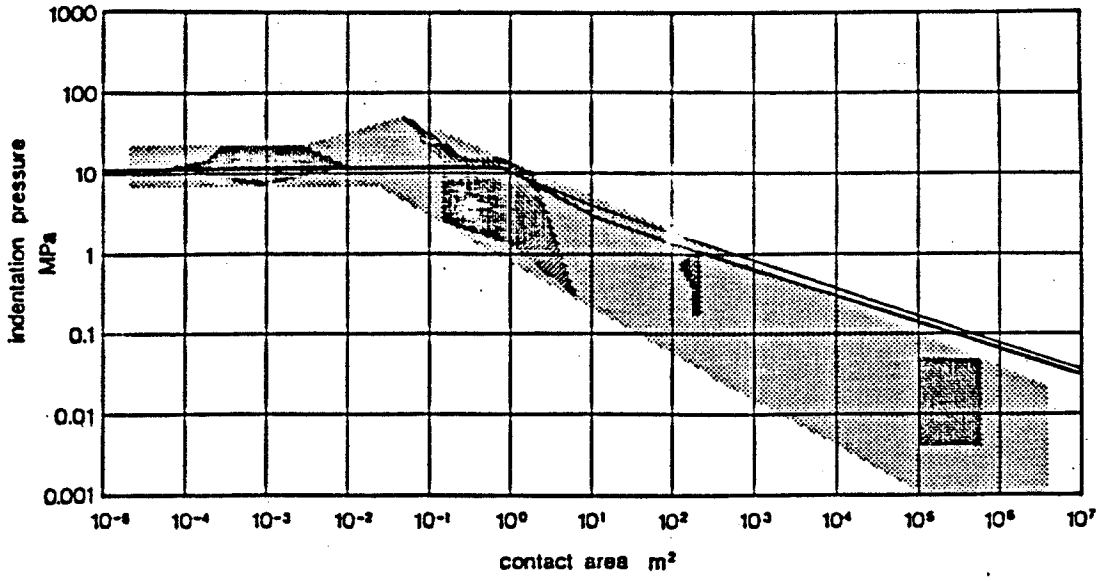

Fig. 4 - Pressure-Area Curve

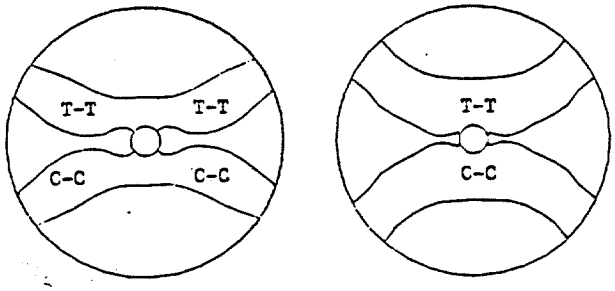

(a) Isotropic Case (β_1=1) (b) Anisotropic Case (β_1=5)

Fig. 5 - Biaxial Stress States at Steady State for Fixed Conditions

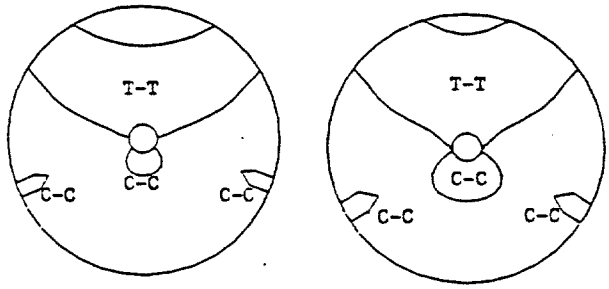

(a) Isotropic Case (β_1=1) (b) Anisotropic Case (β_1=5)

Fig. 6 - Biaxial Stress States at Steady State for Free Condition

insensitive material model was found adequate to describe the first-year sea ice data considered in this paper. Numerical simulations of ice-structure interaction for a rigid cylindrical indenter under plane stress conditions, a problem of general interest for structural concepts in the Arctic, and a transversely isotropic elastic - power law creep model for sea ice showed that:

1. Anisotropy, as represented by the stress ratio β_1 varying between 1 and 5, can cause global forces to increase by almost 15 percent depending upon whether the interface condition is fixed (infinite adfreeze bond strength), roller, or free (no adfreeze bond strength or interface friction). The factor is 1.10 for the fixed condition, 1.12 for the roller condition, and 1.13 for the free condition.
2. Anisotropy can cause maximum (peak) normal interface pressures to increase by almost 20 percent depending upon the interface condition. The factor is 1.07 for the fixed condition, 1.16 for the roller condition, and 1.19 for the free condition. The interface shear stress for the fixed condition essentially remains unchanged.
3. Finite element predictions of global forces and local pressures differ from a (approximate) modified upper bound solution by less than about 10% for varying velocity, indenter diameter, and material constants.
4. Theoretical predictions of pressure-area curves under "breakout" conditions provide an excellent match to measured local pressures.
5. Anisotropy leads to an increase in the size of the compression-compression and tension-tension states of stress on the upstream and downstream sides, respectively, of the indenter.
6. Anisotropy leads to decreasing strains for the roller and free conditions but to almost no change for the fixed condition. This is associated with the increase in lateral confinement near the upstream and downstream tips of the indenter which in turn significantly affects the behavior of transversely isotropic sea ice. Lateral confine-

ment effects are smaller for the fixed condition since the influence of anisotropy is more evenly distributed over the interface due to the presence of interface shear stresses.

The numerical simulations also showed that (i) even a factor of two uncertainty in velocity will affect ice pressures only by about 20-30%, and (ii) the uncertainties in pressures resulting from variability in the degree of anisotropy is approximately two to three times less important than the variability in the reference power law constants a and N. The latter constants can lead to ice strengths varying by a factor of 3-5.

Further research is required to (a) predict the level of force that can be directly transmitted to the foundation by a rubble pile, (b) study the influence of boundary value problems other than "breakout" on pressure-area curves, and (c) study the influence of high confining pressures, temperature gradients, and fracture in problems of ice-structure interaction.

ACKNOWLEDGEMENTS

The authors would like to thank Professor Jerome J. Connor and Mr. Fadi S. Chehayeb, graduate student, for their technical contributions during the course of this work. This research is funded by The Standard Oil Company (Ohio) through MIT's Center for Scientific Excellence in Offshore Engineering, and cosponsored by the U.S. Department of the Interior, Minerals Management Service.

REFERENCES

1. Michel, S. and Toussaint, N., "Mechanisms and Theory of Indentation of Ice Plates," Journal of Glaciology, 19(81), 1977, 285-300.
2. Croasdale, K.R., Morgenstern, M.R. and Nuttall, J.B., "Indentation Tests to Investigate Ice Pressures on Vertical Piers," Journal of Glaciology, 19(81), 1977, 310-312.
3. Ponter, A.R.S. et al., "The Force Exerted by a Moving Ice Sheet on an Offshore Structure: Part I - The Creep Mode," Cold Regions Science and Technology, 8, 1983, 109-118.
4. Bruen, F.J. and Vivatrat, V., "Ice Force Prediction Based on Strain-Rate Field," Proceedings, Third International Symposium on Offshore Mechanics and Arctic Engineering, New Orleans, LA, 3, February 1984, 275-281.
5. Vivatrat, V., Chen, V. and Bruen, F.J., "Ice Load Prediction for Arctic Nearshore Zone," Cold Regions Science and Technology, 1984, 26p.
6. Ting, S-K, and Shyam Sunder, S., "Sea Ice Indentation Accounting for Strain-Rate Variation," Proceedings, ASCE Specialty Conference: ARCTIC '85 - Civil Engineering in the Arctic Offshore, San Francisco, CA, March 1985, 931-941.
7. Chehayeb, F.S., Ting, S-K., Shyam Sunder, S. and Connor, J.J., "Sea Ice Indentation in the Creeping Mode," Proceedings, 17th Annual Offshore Technology Conference, OTC 5056, May 1985, 329-341.
8. Weeks, W.F. and Gow, A.J., "Preferred Crystal Orientations Along the Margins of the Arctic Ocean," Journal of Geophysical Research, 84(C10), 1978, 5105-5121.
9. Langhorne, P.J., "Crystal Alignment in Sea Ice," Ph.D. Thesis, University of Cambridge, U.K., 1982.
10. Langhorne, P.J., "Laboratory Experiments on Crystal Orientation in NaCl Ice," Annals of Glaciology, 4, 1983, 163-169.
11. Cherepanov, N.V., "Spatial Arrangement of Sea Ice Crystal Structure," Prob. Arkt. i Antarki, 38, 1971, 171-181.
12. Kovacs, A. and Morey, R.M., "Investigations of Sea Ice Anisotropy, Electromagnetic Properties, Strength, and Under-Ice Current Orientation," Research Report No. 80-20, U.S. Army Cold Regions Research and Engineering Laboratory, Hanover, NH, 1980, 18p.
13. Butkovich, T.R., "On the Mechanical Properties of Sea-Ice," Research Report RR54, U.S. Snow, Ice and Permafrost Research Establishment, Thule, Greenland, 1959.
14. Peyton, H.R., "Sea-Ice Strength," Research Report No. UAG R-182, University of Alaska, Geophysical Institute, 1966.
15. Vaudrey, K.D., "Ice Engineering - Study of Related Properties of Floating Sea-Ice Sheets and Summary of Elastic and Viscoelastic Analyses," Technical Report R860, Naval Civil Engineering Laboratory, Port Hueneme, CA, 1977.
16. Sinha, N.K., "Field Tests on Rate Sensitivity of Vertical Strength and Deformation of First-Year Columnar-Grained Sea Ice," Proceedings, 7th International Conference on Port and Ocean Engineering Under Arctic Conditions, Helsinki, 1, April 1983, 909-919.
17. Frederking, R., "Ice Engineering I," Lecture Notes, 1983.
18. Wang, Y.S., "Crystallographic Studies and Strength Tests of Field Ice in the Alaskan Beaufort Sea," Proceedings, 5th International Conference on Port and Ocean Engineering Under Arctic Conditions, Trondheim, Norway, 1979, 651-665.
19. Vittoratos, E.S., "Existence of Oriented Sea Ice by the Mackenzie Delta," Proceedings, 5th International Conference on Port and Ocean Engineering Under Arctic Conditions, Trondheim, Norway, 1979, 643-650.
20. Richter-Menge, J.A. et al., "Triaxial Testing of First-Year Sea Ice," Internal Research Report 877, U.S. Army Cold Regions Research and Engineering Laboratory, Hanover, NH, 1985.
21. Peyton, H.R., "Ice and Marine Structures," Ocean Industry, 3(3), March 1968, 40-41; 3(9), September 1968, 59-65; 3(12), December 1968, 51-58.
22. Reinicke, K.M. and Ralston, T.D., "Plastic Limit Analysis with an Anisotropic, Parabolic Yield Function," International Journal of Rock Mechanics, Mining Sciences and Geomechanics, 14, 1977, 147-154.
23. Vivatrat, V. and Chen, V., "Ice Load Prediction with the Use of a Rate-Dependent Anisotropic Constitutive Law," Proceedings, ASCE Specialty Conference: ARCTIC '85 -Civil Engineering in the Arctic Offshore, San Francisco, CA, March 1985, 942-952.
24. Ralston, T.D., "An Analysis of Ice Sheet Indentation," Proceedings, IAHR Ice Symposium, Lulea, Sweden, 1978, 13-31.
25. American Petroleum Institute, "Bulletin on Planning, Designing, and Constructing Fixed Offshore Structures in Ice Environments," Bul. 2N, First Edition, January 1982.
26. Glen, J.W., "The Creep of Polycrystalline Ice," Proceedings, Royal Society of London, Series A, 228(1175), 1955, 519-538.

27. Ganguly, J., "Finite Element Modeling of Sea Ice Indentation in the Creeping Mode," Master of Science Thesis in Civil Engineering, Massachusetts Institute of Technology, Cambridge, MA, January 1986.
28. Ting, S-K., "Constitutive Modeling of Sea Ice with Applications to Indentation Problems," Doctor of Science Thesis in Structural Engineering, Massachusetts Institute of Technology, Cambridge, MA, October 1985.
29. Mellor, M., "Mechanical Behavior of Sea Ice," CRREL Monograph 83-1, U.S. Army Cold Regions Research and Engineering Laboratory, Hanover, NH, 1983, 105 p.
30. Palmer, A.C., "Creep-Velocity Bounds and Glacier Flow Problems," Journal of Glaciology, 6(46), 1967, 479-488.
31. Frederking, R., "Plane Strain Compressive Strength of Columnar-Grained and Granular-Snow Ice," Journal of Glaciology, 18(80), 1977, 505-516.
32. Hausler, F.U., "Multiaxial Compressive Strength Tests on Saline Ice with Brush-Type Loading Platens," Proceedings, IAHR Ice Symposium, Quebec, Canada, July 1981, 526-539.
33. Panoov, V.V. and Fokeev, N.V., "Compression Strength of Sea Ice Specimens under Complex Loading," Problemy Arktiki i Antarktiki, 49, 1977, 81-86 (English Translation, 97-104).
34. Jones, S.J., "Triaxial Testing of Polycrystalline Ice," Proceedings, Third International Conference on Permafrost, Edmonton, Alberta, Canada, July, 1978, 671-674.
35. Jones, S.J., "The Confined Compressive Strength of Polycrystalline Ice," Journal of Glaciology, Vol. 28, No. 98, 1982, pp. 171-177.
36. Reinicke, K.M. and Remer, R., "A Procedure for the Determination of Ice Forces - Illustrated for Polycrystalline Ice," Proceedings, IAHR Ice Symposium, Lulea, Sweden, August 1978, 217-238.
37. Sanderson, T.J.O., "Theoretical and Measured Ice Forces on Wide Structures," Proceedings, IAHR Ice Symposium, Hamburg, August 1984, 32p.
38. Wang, Y.S., "A Rate-Dependent Stress-Strain Relationship for Sea Ice," Proceedings, First International Symposium on Offshore Mechanics and Artic Engineering, New Orleans, LA, 1982, 243-248.
39. Bruen, F.J., Byrd, R.C., Vivatrat, V. and Watt, B.J., "Selection of Local Design Ice Pressures for Arctic Systems," Proceedings, 14th Annual Offshore Technology Conference, OTC 4334, May 1982, 417-435.
40. Sanderson, T.J.O., Personal Communications, 1984.
41. Haynes, F.D., "Tensile Strength of Ice Under Triaxial Stresses," Research Report 312, U.S. Army Cold Regions Research and Engineering Laboratory, Hanover, NH, 1973, 21p.

NOMENCLATURE

a	parameter of power law model in reference direction
a_i	six parameters of orthotropic material model
A	constant equal to a_1+a_2
$\underline{B}$	finite element transformation matrix
$\underline{C}$	linear elastic orthotropic compliance matrix
D	indenter diameter
$\underline{D}$	linear elastic orthotropic rigidity matrix
E	Young's modulus for transversely isotropic sea ice
$\underline{G}$	transformation matrix relating $\underline{S}^*$ to σ
$\underline{K}$	linear elastic stiffness matrix of finite element
$\underline{K}_G$	linear elastic global stiffness matrix
n	constant equal to $2N/(N+1)$
N	power law exponent
P	global force on indenter
$\underline{P}$	applied load vector
$\underline{S}^*$	pseudo deviatoric stress vector for orthotropic material
t	thickness of ice sheet
t_i	time at instant i
$\underline{U}$	nodal displacement vector
$\underline{V}$	approach velocity of ice sheet
α	parameter in time integrator
β_i	five ratios of maximum stress along x, z and the 45° axes on the y-z, x-y and z-x planes, respectively, to the stress in the reference y-direction
Γ	ratios of stresses or pressures under different conditions
$\underline{\varepsilon}$	total strain vector
$\underline{\varepsilon}_c$	creep strain vector
ε_e	effective strainrate measure
θ	plane strain to plane stress conversion factor
λ	associative flow rule constant
ν	Poisson's ratio for transversely isotropic sea ice
$\underline{\sigma}$	stress vector
σ_e	effective stress measure
τ	ratio of confining pressure to axial stress
ϕ	scalar potential function
$\dot{\ }$	rate form is represented by a dot above the symbol